



Soil quality dynamics across a landslide profile from intact slopes to displaced material and bedrock

Gheorghe Roşian¹, Ramona Bălc¹, Roxana Moga¹, Ştefan Șfabu¹, Tudor Osiescu¹, Csaba Horvath², Tiberius Dicu¹

⁵ ¹Faculty of Environmental Science and Engineering, Babes-Bolyai University, 400294 Cluj-Napoca, Romania

²Faculty of Geography, Babes-Bolyai University, 400294 Cluj-Napoca, Romania

Correspondence to: Ramona Bălc (ramona.balc@ubbcluj.ro)

Abstract. Landslides modify soil systems by disrupting pedogenic processes, altering physical structure, and redistributing chemical constituents. To assess these effects and address key knowledge gaps, this study examines soil quality dynamics along a geomorphological transect crossing intact slopes, displaced landslide material, and parent substrate in the Transylvanian Basin. A suite of physico-chemical, together with magnetic parameters, considered herein as a previously underutilized yet promising proxy for soil degradation, was analysed to identify the soil properties most affected by landsliding, test for statistically significant contrasts between disturbed and undisturbed soils, and determine the most reliable indicators of soil degradation. Magnetic properties showed the clearest diagnostic response: mass-specific and frequency-dependent susceptibility were markedly reduced within the landslide, reflecting the removal or mixing of magnetically enriched horizons. Landslide-affected soils exhibited higher bulk density, lower organic matter, elevated electrical conductivity, and homogenized clay patterns compared with intact profiles. These results demonstrate that landslides profoundly alter soil composition and structure, and highlight magnetic susceptibility, organic matter, and electrical conductivity as robust indicators for assessing disturbance severity. The findings provide a comprehensive framework for evaluating soil degradation in landslide-prone environments.

1 Introduction

The functioning of terrestrial ecosystems and the delivery of key ecosystem services critically depend on the capacity of soil to maintain favourable physical, chemical and biological properties (Doran and Zeiss, 2000). Soil quality, defined as “the ability of a particular soil to function within natural or managed ecosystems to sustain productivity, maintain environmental quality, and promote plant and animal health” (Doran and Parkin, 1996), is sensitive to geomorphological disturbances such as mass-wasting events. Among these, landslides represent a major driver of soil system perturbation because they remove or displace developed soil horizons, expose parent material (Geertsema et al., 2009), disrupt vegetation cover (Blońska et al., 2018), and thus reset pedogenic and biogeochemical processes. Landslide-affected landscapes are therefore important for



30 investigating how soil quality respond to disturbance, how pedogenesis and recovery proceed, and how soil functions evolve spatially from intact terrain through the disturbed zone to underlying bedrock.

From a pedological and geomorphological perspective, landslides alter the vertical and lateral continuity of soil formation and cause abrupt transitions in soil properties. For instance, the removal of the organic-rich A horizon and mixing of mineral horizons leads to reductions in soil organic carbon (SOC), microbial biomass and enzyme activity (Blońska et al., 2018).

35 Physical structure is also degraded: bulk density may increase, porosity decline, and horizon differentiation may be lost, leading to poorer aggregate stability (Goyal et al., 2022). Chemically, the exposure of the fresh mineral surfaces and disruption of biogeochemical cycling may reduce nutrient stocks (available N, P, K) and alter pH, cation exchange capacity and other soil reactivity parameters (Goyal et al., 2022; Cerri et al., 2020). Despite this, the interface between landslide geomorphology and soil quality dynamics remains under-explored, particularly regarding full landslide profiles spanning intact slopes, the
40 displaced material (transport and accumulation zones), and exposed bedrock.

Existing studies have documented soil property gradients in disturbed zones and chronicled the recovery of soil quality over time. For example, Goyal et al. (2022) used a chronosequence of landslides in the Indian Himalayas to show that SOC, available P and clay fraction progressively improve with landslide age, reaching ~84-97% of undisturbed reference levels after ~26 years. Likewise, Blońska et al. (2018) investigated a landslide in the Polish Carpathians and identified strong spatial
45 variability of physical, chemical and biochemical properties within the slide, with the least developed soil cover in the head niche zone. Meanwhile, Cerri et al. (2020) examined soil cover along Brazilian Atlantic coast and revealed that soil architecture (e.g., microporosity, mottles) and mineralogical features condition slope movement and pedogenesis. These studies highlight that soil quality degradation and partial restoration occur following mass-wasting, yet the continuity of change across intact-displaced-bedrock segments of a landslide profile remains rarely quantified.

50 Critically, there is a gap in understanding how the entire landslide profile, from intact slope through displaced soil masses to exposed bedrock, operates as a continuum of soil quality dynamics. Most work focuses either on the displaced zone or on post-disturbance recovery in isolation; few integrate intact, displaced and bedrock zones in a single conceptual and analytical framework. Moreover, the simultaneous assessment of physical, chemical and biological indicators across such a profile is relatively uncommon. This has implications not only for pedogenetic theory and landscape ecology, but also for practical
55 issues such as slope restoration, soil fertility recovery and hazard mitigation.

To address the identified knowledge gaps, this study integrates soil quality dynamics across a complete landslide profile within the Transylvanian Basin. Sampling was conducted along a geomorphological transect encompassing intact slope positions, displaced material (transport and accumulation zones), and exposed bedrock or subsoil strata, in order to capture spatial
60 gradients in soil physical and chemical indicators. The specific objectives of the research are to: (i) identify the soil physico-chemical parameters most significantly affected by landslide activity; (ii) assess whether statistically significant differences in soil properties exist between landslide-affected and unaffected areas; and (iii) determine the most diagnostically relevant soil attributes that can serve as reliable indicators for evaluating the extent and severity of soil degradation. Hypothesized that soil quality will progressively decline from intact slope through displace material to bedrock exposure, reflecting disturbance and



pedogenic resetting while the displaced material will display intermediate characteristics due to partial recovery or horizon mixing. By integrating diverse soil quality indicators, this study aims to develop a robust framework for discriminating geomorphic zones and elucidating the processes governing soil system evolution in slope-failure context.

2 Materials and methods

2. 1 Study area

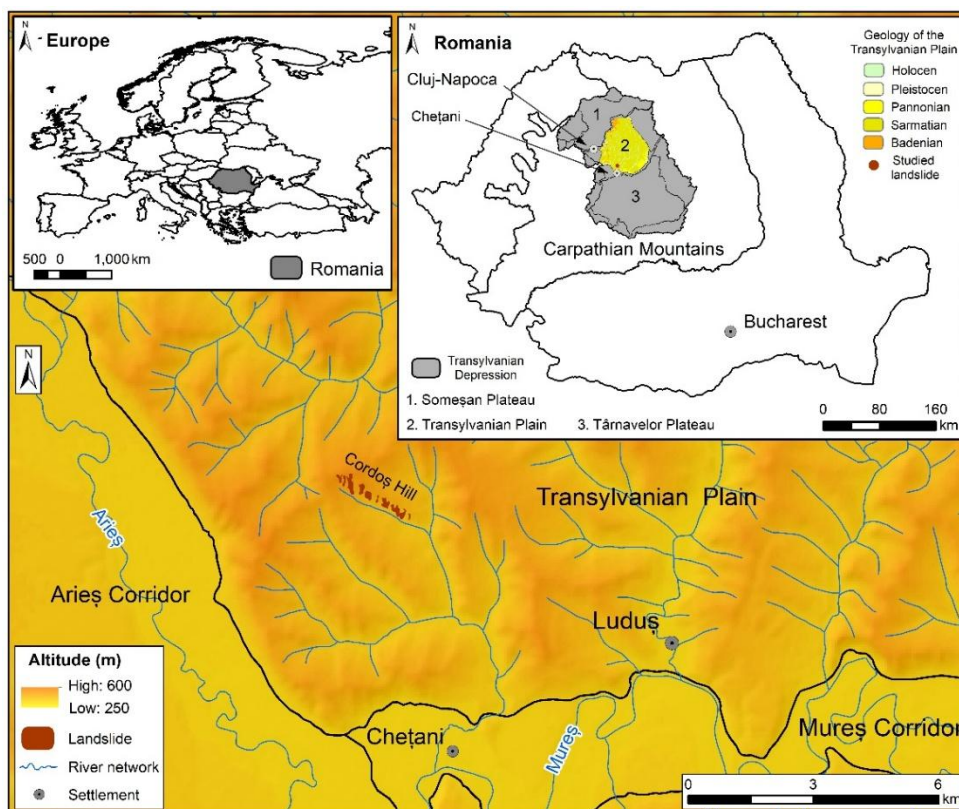
The study area is situated within the Transylvanian Basin, a morphostructural unit comprising three principal subunits, 70 complemented by the submontane hills and depressions. From north to south, corresponding to the surface distribution of geological formations, the main morphostructural units are the Someş Plateau, the Transylvanian Plain, and the Târnava Plateau (Fig. 1). At the regional scale, the landslide is located within the morphostructural subunit known as the Transylvanian Plain. Administratively, it falls within the Chețani Territorial Administrative Unit (commune of Chețani), Mureş County. The geographic coordinates of the site are 46°31'06" N latitude and 24°00'08" E longitude. More specifically, the landslide is 75 positioned in the central-western sector of the Transylvanian Basin, on the left slope of the Cordoş Valley (Fig. 1 and 2). The Cordoş stream, which drains this valley, is a tributary of the Grindeni River, which in turn flows into the Arieş River.

The Transylvanian Basin constitutes a key sedimentary province situated in the southeastern segment of the Carpathian orogenic belt (Fig. 1). Its stratigraphic infill encompasses a succession of deposits spanning the Upper Cretaceous to the Pliocene (Huismans et al., 1997). Basin development is conventionally subdivided into four principal evolutionary phases, 80 each expressed by discrete tectonostratigraphic megasequences: (1) a Late Cretaceous syn-rift episode; (2) a Paleogene post-rift sag phase; (3) an early Miocene flexural stage associated with peripheral loading; and (4) a middle to late Miocene-Pliocene back-arc basin phase (Krézsek and Bally, 2006). Upper Cretaceous sedimentary assemblages comprise conglomerates, sandstones, marls, and rudist-bearing limestones deposited across a spectrum of continental, shallow-marine, and deep-marine settings (Paraschiv, 1979; de Broucker et al., 1998). These units overlie a basement complex that underwent significant 85 deformation prior to and during the Early Cretaceous. The maximum accumulation of these deposits occurs in the western sector of the basin, where coarse clastic lithofacies predominate (Ciulavu and Bertotti, 1994).

The Miocene development of the Transylvanian Basin was fundamentally governed by geodynamic processes associated with the terminal phases of subduction along the Carpathian arc (Săndulescu, 1984; Royden, 1988; Săndulescu, 1988; Ciulavu et al., 2000; Sanders et al., 2002). The Early Badenian is marked by the accumulation of deep-marine siliciclastic turbidites within 90 the central sector of the basin, whereas mixed shelfal and coastal deposits developed along its margins (Ciupagea et al., 1970; Krézsek and Bally, 2006; Krézsek et al., 2007). By the middle Badenian, hydrological isolation of the basin had been established, promoting the precipitation of halite in deeper marine settings and the formation of shallow-water to sabkha-type gypsum along the peripheral zones (Ciupagea et al., 1970; Krézsek and Bally, 2006). Although tectonic deformation continued from the late Miocene through Pliocene, the most significant phases of diapiric activity occurred during the late Sarmatian to 95 Pannonian interval. The Sarmatian interval is mainly represented by siliciclastic deposits, but it also encompasses carbonate



and evaporitic facies, particularly toward the basin margins (Krézsek and Filipescu, 2005; Krézsek and Bally, 2006). In the basin's central domain, Sarmatian strata reach thicknesses greater than 1000 m (Krézsek and Filipescu, 2005).



100 **Figure 1. Location of the studied landslide within Europe and Romania. The map highlights the position of the study area within the broader European context and shows its precise location within Romania. Elevation features are included to illustrate the landscape setting of the landslide-affected area investigated in this study.**

105 Sarmatian deposits in the Transylvanian Basin, composed predominantly of marls and clays rich in swelling clay minerals such as montmorillonite, illite, and beidellite, exhibit a high predisposition to slope instability (Ciupagea et al., 1970; Matei, 1983). The susceptibility of these fine-grained units to landsliding is further influenced by a suite of geomorphological and anthropogenic factors, including slope gradient, slope aspect, and land-use practices (Roşian et al., 2016; Bălteanu et al., 2020). The landscape developed on Sarmatian formations is predominantly of fluvial origin, characterized by widespread slopes ranging between 5° and 25°, which commonly host numerous gravitational slope-deformation processes.

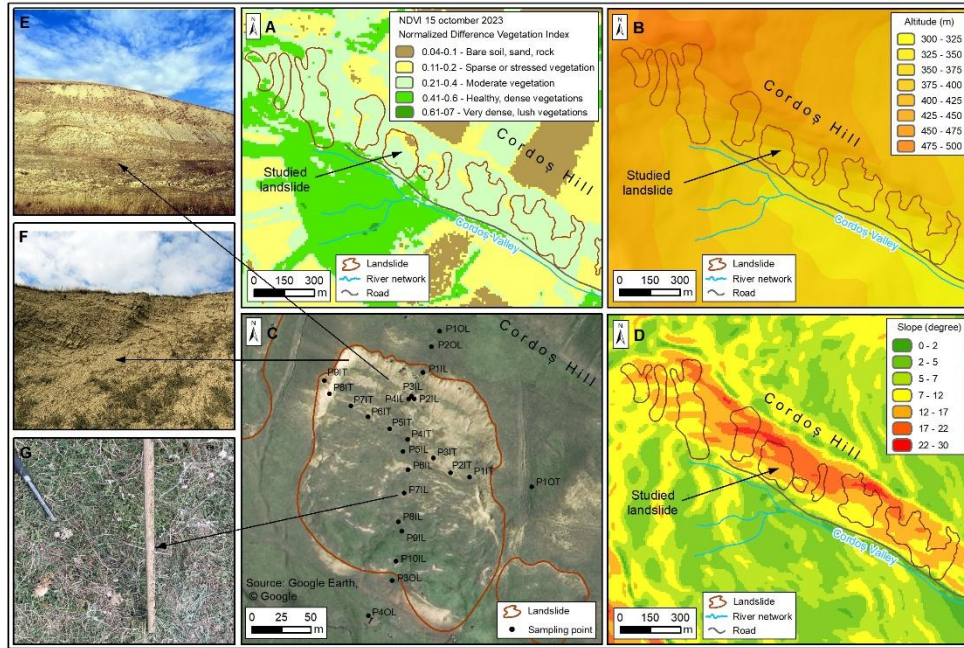


Figure 2. Overview of the landslide area in Cordoș Valley, Transylvanian Basin, integrating remote sensing, aerial imagery, and field observations: (A) NDVI map (15 Oct. 2023) showing vegetation density (0.04-0.7) and the landslide outline; (B) DEM-based altitude map (200-500 m) indicating the topographic context; (C) Orthophoto with sampling points illustrating field strategy (Google Earth); (D) Slope map (0-30°) highlighting landslide concentration on steeper slopes (12-30°); (E-G) Field photographs of the landslide: wide view (E), exposed parent rock (F), and detailed view of the landslide core (G).

The landslide is a simple rotational type (single rotational slide), according to the classification proposed by Cruden and Varnes (1996). The investigated landslide most likely occurred around 1970, as it is depicted on the 1972 edition of the Topographic Map of Romania. The elevation difference between the upper part (435 m a.s.l.) and the lower part (340 m a.s.l.) of the left slope of the După Vii Valley is approximately 95 m. The slope gradient ranges from about 7° in the lower sector to 24° in the upper sector, where the main scarp of the landslide is located. Within the landslide body, slope gradients vary between 7° and 17°. Both the slope and the landslide body have a southern exposure. The main scarp is situated at an elevation of 410 m, while the lower, stabilized portion lies at approximately 347 m. Over this elevation of 63 m, the landslide extends for a total length of 298 m. The feature has an average width of 174 m and occupies an area of about 36.567 m² (equivalent to 0.036 km² or 3.65 ha). Based on these dimensions and the observed morphology of the displaced mass, the estimated thickness (depth) of the landslide ranges between 8 and 10 m. In the absence of borehole data, the volume can be approximated as the product of length, width, and depth, yielding an estimated value of approximately 351 000 m³.

Landslide surface is predominantly covered by moderate to sparse vegetation, with 93% of values below 0.40. Approximately 24% of the area corresponds to stressed or sparse vegetation, and 7% of it indicates nearly bare soil, suggesting limited ground cover and active erosion. Only 0.3% of the surface exhibits dense vegetation, and woody or stable cover is virtually absent



(<1%), highlighting an unstabilized, recently reworked geomorphic surface. This NDVI pattern reflects the early recovery stage of vegetation following landslide activity and confirms the high environmental sensitivity of the area within the Plain of 135 Transylvania (Fig. 2A).

2. 2 Soil sampling and analysis

Soil samples were collected from the upper 60 cm along two transects, one longitudinal and one transversal, following the transition zone between undisturbed and disturbed areas (Fig. 2C). Five sampling points (P1OL-P4OL, P1OT) were selected as reference sites located outside the landslide area. A total of nineteen sampling points (P1L-P10L and P1T-P9T) were 140 established within the landslide mass, while fourteen samples (P1-P14) were collected from bedrock exposures on the left side of the landslide, near the main scarp, in the zone of maximum slope inclination. Except for the bedrock samples, all soil samples were collected from three depth intervals: 0-20 cm, 20-40 cm and 40-60 cm. The sampling design employed in this study has several limitations that should be acknowledged. First, soil samples were collected along only two transects, which 145 may not fully capture the spatial variability of soil and lithological properties across the entire landslide and adjacent undisturbed areas. The upper 60 cm sampling depth provides information on the most active soil layer but does not account for processes occurring at greater depths that may influence landslide dynamics or subsurface hydrology. In addition, the sampling campaign represents a single temporal snapshot, and potential seasonal or post-event variations in soil moisture and geochemical characteristics were not assessed. The uneven distribution of sampling points among reference sites landslide 150 material, and bedrock exposures may also introduce a degree of statistical imbalance. Furthermore, differences in the nature of the collected materials, limit the direct comparability of their physical and chemical parameters. Despite of all these, the sampling strategy provides a solid basis for analysing soil and substrate variability within and around the landslide area. The combination of longitudinal and transversal transects captures both along-slope and cross-slope variations, while reference sites enable clear comparison between disturbed and undisturbed conditions. Sampling at three depth intervals allows assessment of vertical heterogeneity within the active soil layer, and the inclusion of bedrock samples supports interpretation 155 of lithological influences on slope processes. Overall, the systematic design ensures representative coverage of key geomorphological zones and strengthens the reliability of spatial and comparative analyses.

The soil samples were analyzed for their physical and physico-chemical parameters as follows: bulk density, clay content, pH, electrical conductivity (EC), organic matter (OM) and magnetic susceptibility (MS). The dry soil bulk density (ρ_b) was calculated using the formula:

$$160 \quad \rho_b = \frac{md}{V} \quad (1)$$

where ρ_b is in g m^{-3} , md is the mass of the sample dried at 105°C in grams g, and V is the volume of the steel cylinder in cubic centimetres cm^3 (ISO 11272:2017).

Sediment texture was assessed using the standard hydrometer method (Forth, 1991) in accordance with current national standards (STAS 1913/5-85 and SR EN 14688-2, 2005). Samples were classified into four fractions based on particle size:



165 clay (< 0.002 mm), silt (0.002-0.063 mm), sand (0.063-2 mm), and gravel (2-63 mm). This procedure combines sedimentation for fine particles with sieving for coarser fractions. The resulting proportions of each size class were plotted on a ternary diagram, which includes 12 major textural categories, allowing the conversion of grain size distributions into standard sediment texture types.

170 Physico-chemical parameters, pH and EC, were measured using a multimeter (Multi 3320, WTW, Germany) equipped with a pH electrode (SenTix 41, WTW, Germany), and a conductivity cell (TetraCon 325, WTW, Germany). Soil pH and EC were measured in aqueous solution obtained by mixing 50 g of dry soil with 200 ml of distilled water and shaking the suspension for 90 min. After allowing it to settle for an additional 15 min, the pH and EC of the supernatant were measured using the pH and EC electrodes.

175 Organic matter was determined using the basic Loss on Ignition method (Heiri et al., 2001). After oven-drying the soil to constant weight (typically 12-24 hours at approximately 105°C), organic matter was combusted to ash and carbon dioxide at 550°C. The loss on ignition (LOI) was then calculated as follows:

$$LOI_{550} = \frac{DW_{105} - DW_{550}}{DW_{105}} \times 100 \quad (2)$$

180 Where LOI_{550} is the percentage weight loss at 550°C, DW_{105} is the dry weight of the sample before combustion, and DW_{550} is the dry weight after heating to 550°C. The weight loss is assumed to be proportional to the organic carbon content of the sample, and Dean (1974) demonstrated a strong correlation between LOI_{550} and organic carbon measured chromatographically. Magnetic susceptibility (MS) was analyzed using a Bartington magnetic susceptibility meter (MS2) equipped with a dual-frequency sensor (MS3). The specific volumetric magnetic susceptibility (κ) was measured at low (0.47 kHz; κ_{lf}) and high (4.7 kHz; κ_{hf}) frequencies. Bulk density (ρ) was calculated as the ratio of sample mass to volume. The mass-specific susceptibility (χ) is proportional to the concentration of ferrimagnetic minerals, primarily magnetite and maghemite. Low-frequency susceptibility (χ_{lf}) was calculated as (Bouhsane and Bouhassa, 2018):

$$\chi_{lf} = \frac{\kappa_{lf}}{\rho} \quad (3)$$

The frequency-dependent susceptibility (χ_{fd}) was determined either as absolute loss of susceptibility:

$$\chi_{fd} = \chi_{lf} - \chi_{hf} \quad (4)$$

or as percentage, referred to as the percentage frequency-dependent susceptibility ($\chi_{fd\%}$):

$$190 \chi_{fd\%} = \frac{\chi_{lf} - \chi_{hf}}{\chi_{lf}} \times 100 \quad (5)$$

where χ_{lf} and χ_{hf} correspond to the susceptibilities measured at low and high frequencies, respectively. The percentage frequency dependence reflects the relative contribution of superparamagnetic (SP) and stable single-domain (SSD) particles to the total magnetic signal. Additionally, χ_{fd} can be used to estimate the concentration of fine magnetic grains exceeding the SP/SD size limit.



195 2. 3 Statistical elaboration and image analysis

Descriptive statistical indicators, including minimum (min), maximum (max), mean, and standard deviation (SD), were computed for each variable measured in the soil samples using Microsoft Excel. These statistics provide an overview of the data tendency and dispersion and support the reader in visualizing the dataset.

200 To analyze the variation among the target groups, a one-way ANOVA test was applied using GraphPad Prism software. This test compares the means of three or more independent groups to determine whether at least one group differs significantly from the others (Ross and Willson, 2017). In the present study, the target groups were defined based on the sampling location—outside the landslide, within the landslide body, and the parent rock—as well as the depth from which the samples were collected (surface, 0–20 cm, 21–40 cm, or 41–60 cm).

205 The Normalized Difference Vegetation Index (NDVI) was derived from Sentinel-2 L2A imagery acquired on 15 October 2023, selected for its low cloud cover (<5%) and optimal post-summer vegetation conditions. The NDVI was calculated using the standard formula $NDVI = (B8 - B4) / (B8 + B4)$, where B8 (NIR) represents the near-infrared band and B4 (Red) the red band reflectance. Prior to processing, the image underwent atmospheric correction and cloud masking based on the Scene Classification Layer (SCL) to ensure high data reliability. The resulting NDVI raster was reclassified into five vegetation density classes, ranging from bare soil (0.00–0.10) to very dense vegetation (0.61–0.70), reflecting the spectrum from degraded 210 surfaces to lush vegetative cover. Spatial analyses were conducted in a GIS environment, where zonal statistics were applied to the landslide polygon to determine the areal proportion of each NDVI class.

3 Results

215 The results provide a detailed characterisation of the bulk density across the studied soil samples (Table 1). Soils located outside the landslide exhibit bulk density values ranging from 1.13 to 1.76 g/cm³, with generally lower values in the surface horizon (0-20 cm) than inside the landslide, particularly in surface soils. In contrast, soils within the landslide display consistently higher bulk densities, reaching up to 2.07 g/cm³ at deeper layers (e.g., P2L at 40-60 cm). The parent material exhibits a bulk density around 1.90-1.99 which is expected for unweathered or weakly developed lithological material, characterized by a lack of pedogenic structure and high mineral content. Outside the landslide, the bulk density increases with depth, being consistent with natural compaction and lower organic matter at depth. A very similar pattern is observed within 220 the landslide but often starts shallower than in undisturbed soils, suggesting initial compaction from the landslide. Parent material has a bulk density with more uniform values across the samples.

pH values outside landslide are relatively stable across the samples and depths, mostly between 8.2-9.0, indicating moderately to strongly alkaline conditions. Similar alkaline conditions, though slightly lower in some deeper samples (e.g. P6L, 40-60 cm: pH - 7.9) were identified for the samples collected inside the landslide. Additionally, a decrease of pH values with depth was 225 observed inside landslide. Parent material has a pH which range from 6.8 to 8.7, averaging slightly lower values than both surface soils.



Clay content exhibited substantial variability across depths and sampling locations outside the landslide, ranging from 40.00% to 67.18%, with a slight but consistent increase with depth. The topsoil displayed the greatest heterogeneity, reflecting the influence of pedogenic processes and surface disturbance. Within the landslide zone, clay content was somewhat less variable, 230 yet tended to decrease in the deeper layers, likely due to the mixing of materials with differing granulometric signatures during mass movement. In contrast, the parent material showed comparatively uniform clay values (approximately 35-50%), indicating a more uniform textural composition. Overall, soil texture was relatively consistent across the study area: 51% of the were classified as clay, 46% as sandy clay, and only 3% as silty clay, suggesting that fine-textured soils dominate the investigated profiles regardless of landslide influence.

235

Table 1. Values of measured parameters across sampling site

Samples	Bulk density (g/cm ³)			pH			Clay (%)		
	0-20	20-40	40-60	0-20	20-40	40-60	0-20	20-40	40-60
P1OL	1.36	1.28	1.42	8.2	8.3	8.3	44.80	48.00	51.19
P2OL	1.13	1.54	1.54	8.2	8.5	8.7	55.03	46.40	51.74
P3OL	1.52	1.76	1.67	8.1	8.5	9.0	40.00	48.64	51.16
P4OL	1.58	1.82	1.92	8.2	8.3	8.6	43.84	54.39	67.18
P1OT	1.66	1.74	1.86	8.2	8.2	8.4	41.60	47.68	60.79
P1L	1.62	1.69	1.82	7.9	8.1	8.1	36.80	45.98	39.91
P2L	1.52	1.97	2.07	8.3	8.6	8.4	38.95	59.83	31.27
P3L	1.67	1.98	2.05	7.9	8.3	8.0	44.80	45.66	38.69
P4L	1.62	1.8	1.8	8.1	8.4	8.2	47.96	37.03	40.29
P5L	1.66	1.74	1.62	8.2	8.3	7.9	36.39	43.2	29.45
P6L	1.62	1.67	1.86	7.7	7.9	8.4	56.66	50.87	40.00
P7L	1.82	2.02	2.01	7.9	8.4	8.4	44.80	52.79	46.40
P8L	1.7	1.89	1.76	8.3	8.2	8.2	49.50	41.19	42.24
P9L	1.21	1.57	1.72	8.2	8.2	8.1	36.80	41.57	47.96
P10L	1.54	1.74	1.66	8.3	8.0	8.1	40.67	51.42	51.19
P1T	1.74	1.76	1.84	7.6	8.0	8.4	48.67	48.22	45.02
P2T	1.67	1.7	1.84	8.0	8.3	8.0	41.60	46.62	55.32
P3T	1.87	1.99	1.8	8.1	8.3	8.2	53.46	41.19	36.77
P4T	1.76	1.83	1.9	8.2	8.4	8.4	37.73	44.38	43.20
P5T	1.68	1.8	1.83	8.0	8.1	7.5	33.83	41.82	49.59
P6T	1.65	1.92	1.84	8.0	8.1	7.9	44.80	41.82	41.89



P7T	1.67	1.63	1.66	8.3	8.0	8.1	44.80	46.11	49.31
P8T	1.65	1.72	1.53	7.8	8.0	8.0	59.16	51.87	45.66
P9T	1.3	1.38	1.7	8.3	8.2	8.1	44.77	57.59	45.47
P1	1.98			8.3			37.35		
P2	1.98			8.6			38.95		
P3	1.94			7.0			19.44		
P4	1.97			8.7			38.95		
P5	1.89			7.0			34.15		
P6	1.92			8.4			48.96		
P7	1.94			7.0			39.59		
P8	1.91			7.0			42.14		
P9	1.99			6.8			53.66		
P10	1.92			7.1			41.19		
P11	1.92			7.1			50.46		
P12	1.93			7.1			47.26		
P13	1.93			7.1			40.00		
P14	1.92			7.1			43.74		

A brief interpretation of the data obtained for the above presented parameters can be seen in Table 2.

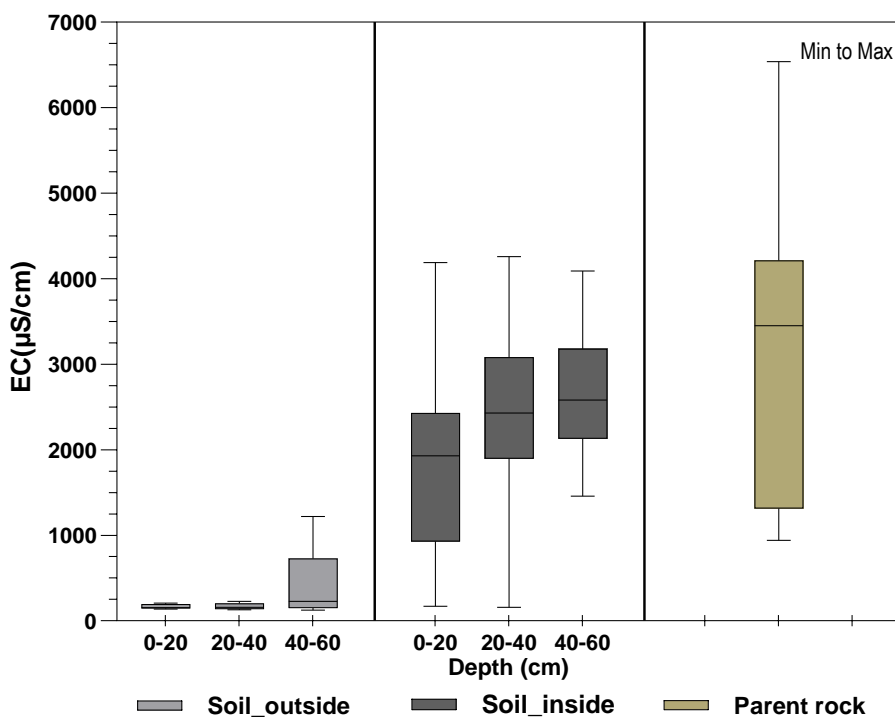
240 **Table 2.** Summary of key findings for bulk density, pH, and clay content

Parameter	Outside the landslide	Inside the landslide	Parent material
Bulk density	Low to moderate; increases with depth	Higher overall	High
pH	Alkaline; stable	Slightly lower in deeper samples	Slightly more variable
Clay	Variable, can increase with depth	Often reduced at depth	Fairly stable

The electrical conductivity (EC) of the soil varied significantly at different landscape positions and depths (Fig. 3). Outside the landslide the values of this parameter are generally low to moderate (between 121.8 µS/cm and 239.0 µS/cm, with the 0-20 cm depth showing the lowest median. A clear increasing trend with depth can be outlined, from low surface values to higher



245 conductivity in deeper layers. Inside the landslide electrical conductivity is consistently higher than outside (between 172.2 $\mu\text{S}/\text{cm}$ and 4260 $\mu\text{S}/\text{cm}$), across all depths ($p < 0.05$) and is more uniform with depth, with a slightly fluctuations but less pronounced than in stable soil. At 0-20 cm and 20-40 cm soil EC show similar values, indicating less distinct stratification, which is expected in mixed or homogenized profiles. The highest EC found among the parent material samples (6540 $\mu\text{S}/\text{cm}$) was significantly different from both inside and outside soil samples ($p < 0.001$), highlighting its role as a salt-rich source of
250 ions. The boxplot also revealed narrower interquartile ranges in the parent material, indicating higher chemical uniformity, whereas landslide soils showed some variability, likely due to mixing processes. These findings underscore the impact of mass movement on soil structure and solute distribution, disrupting natural gradients and increasing salt accumulation in affected profiles.



255 **Figure 3. Boxplot of soil electrical conductivity (EC) across different sampling positions and depths: outside the landslide (grey), inside the landslide (black), and parent material (olive).**

Based on Richards (1954) most of the samples collected from outside the landslide (except for P2OL 40-60 cm) along with
260 three samples collected inside the landslide fall into the low salinity category, while all others can be integrated within the categories of high and very high salinity.

The content of soil organic matter varied significantly across sampling locations and depths (Fig. 4). Soil samples collected outside the landslide area (grey bars), across all three sampling depths, showed the highest levels of organic matter (8.38%,



6.85%, and 7.55%). A clear decreasing trend with depth was observed, with the highest concentration in the topsoil (0–20 cm) and progressively lower values in deeper layers ($p < 0.0001$) between all depth intervals.

265 In contrast, soil collected within the landslide zone (black bars) exhibited significantly reduced organic matter content (maximum of 6.87%) at all sampled depths compared to the corresponding external profiles ($p < 0.0001$). The parent material (olive bar), representing the unweathered or partially weathered geological substrate, had the lowest organic matter content overall (4.12%), which was significantly different from all other samples ($p < 0.0001$). This confirms its minimal contribution to organic matter and supports its role as a baseline for comparison.

270

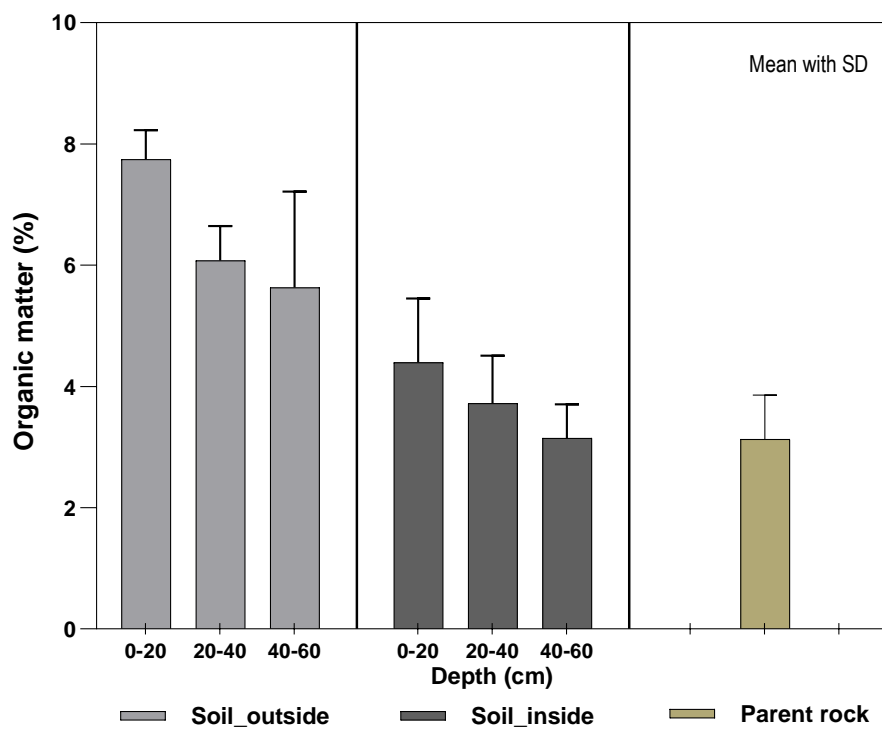


Figure 4. Boxplot of soil organic matter (OM) across different sampling positions and depths: outside the landslide (grey), inside the landslide (black), and parent material (olive).

275 The variation of mass-specific magnetic susceptibility at low frequency is illustrated in Fig. 5. MS values outside the landslide are notably high across all three depth intervals, with a clear decreasing trend with depth: $\sim 80 \times 10^{-8} \text{ m}^3/\text{kg}$ (0-20 cm), $\sim 75 \times 10^{-8} \text{ m}^3/\text{kg}$ (20-40 cm), and $\sim 60 \times 10^{-8} \text{ m}^3/\text{kg}$ (40-60 cm). The relatively large standard deviations, especially in the top 40 cm, imply some heterogeneity in magnetic properties, likely reflecting micro-variations in lithology, organic content, or degree of pedogenic alteration.



280

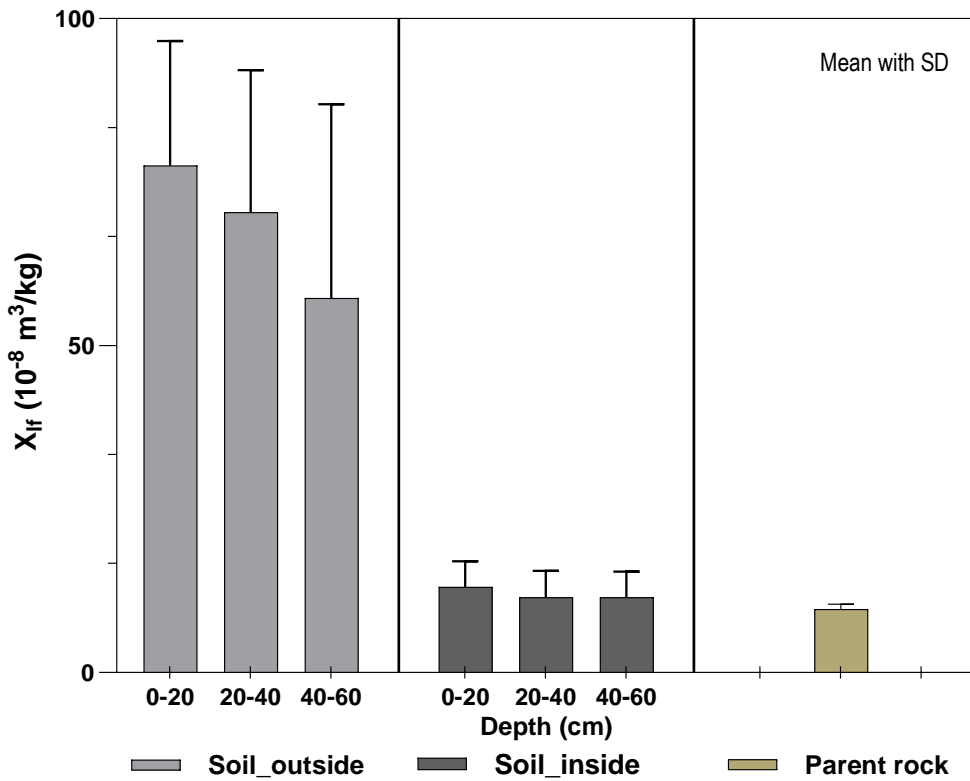


Figure 5. Mean values of mass-specific magnetic susceptibility of soil samples collected from three different depths (0-20 cm, 20-40 cm, and 40-60 cm), across three distinct sample categories.

285 The samples collected inside the landslide exhibit consistently low magnetic susceptibility values, relatively uniform across all depths ($\sim 15 \times 10^{-8} \text{ m}^3/\text{kg}$). The lack of significant vertical variation suggests a homogenized soil profile, likely resulting from mass movement processes associated with the landslide event. This mechanical disturbance may have led to the mixing of topsoil and subsoil, causing the dilution or removal of magnetically enriched surface materials. Additionally, the consistently 290 low susceptibility values could indicate either limited pedogenic enhancement or a dominance of lithogenic (parent material-derived) magnetic minerals with minimal alteration since the landslide event. Compared to the outside-soil profile, these findings imply a resetting or halt of pedogenic processes induced by landslide activity.

The magnetic susceptibility of the parent material is significantly lower ($\sim 10 \times 10^{-8} \text{ m}^3/\text{kg}$) than that of soil from outside and inside the landslide. This value represents the baseline lithogenic contribution of magnetic minerals prior to any pedogenic modification. The low magnetic susceptibility values suggest that the parent material is relatively poor in ferromagnetic 295 minerals and confirm that pedogenesis is responsible for the elevated susceptibility in the outside soils.



Thus, the soils outside the landslide display the highest magnetic susceptibility values which decrease with depth, an archetypal signature of a mature and stable pedogenic system. In contrast, soils inside the landslide present lower and relatively uniform susceptibility values, indicative of disrupted soil formation and magnetic dilution due to landslide dynamics. The parent rock exhibits minimal magnetic susceptibility, reinforcing the conclusion that pedogenic processes are essential in generating 300 magnetic enhancements in surface soils. Overall, the data clearly demonstrate the impact of landslide-induced geomorphological disturbance on soil magnetic properties, with important implications for landscape evolution, soil development, and environmental magnetism studies.

The ANOVA test indicates statistically significant differences ($p < 0.05$) between the three groups (Fig. 6): at 0-20 cm, outside soil has significantly higher mass-specific magnetic susceptibility than soil inside the landslide and the parent material; at 305 20-40 cm, the same pattern holds – outside soil is significantly enriched compared to the other two; and at 40-60 cm, the trend continues, although the magnetic susceptibility values decline slightly with depth, reflecting less pedogenic influence deeper in profile. The presence of “ns” suggests that in the deeper soil layers (20-60 cm), the soil inside the landslide is similar in magnetic properties to the parent material. This implies that the pedogenic enhancement of magnetic minerals is minimal or absent in these disturbed soils. All these findings support the conclusion that landslide activity has disrupted the soil formation 310 process, especially by removing or mixing the magnetically enriched topsoil, resulting in values similar to the unaltered parent rock.

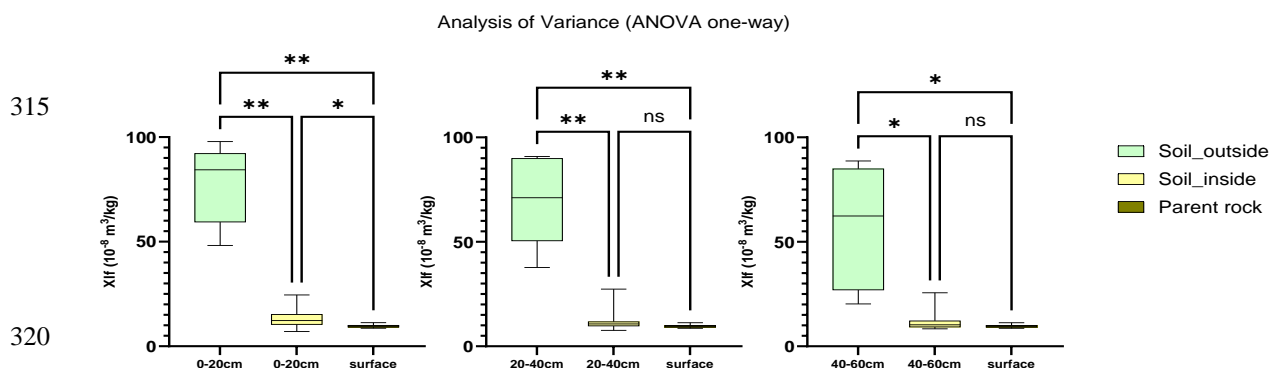


Figure 6. ANOVA test illustrating the statistically significant differences between the analyzed soil samples, showing how their magnetic susceptibility values vary across groups.

The frequency-dependent magnetic susceptibility ($\chi_{fd} \%$) indicates the proportion of superparamagnetic (SP) particles in the 325 soil, typically formed during pedogenesis. High values are associated with well-developed soils and biologically active environments, while low or negative values often indicate disturbed, truncated, or immature soils, and/or the presence of geological material like parent rock. This parameter has high values in soil outside the landslide (Fig. 7), indicating an undisturbed soil profile, where pedogenesis leads to the formation of SP minerals concentrated near the surface. In soil samples collected inside the landslide the frequency-dependent magnetic susceptibility value is much lower at all depths, suggesting



330 that the landslide processes have likely disrupted or removed the SP-rich upper horizons. The soil here shows limited pedogenic development or mixing with deeper, less weathered materials, reducing the frequency-dependent magnetic susceptibility. The parent rock exhibits negative values for this parameter, indicating the absence of SP minerals and the dominance of large ferrimagnetic grains and/or abundant diamagnetic minerals. This pattern is expected for unaltered geological material, the frequency-dependent magnetic susceptibility being negligible or absent. The parent material is magnetically stable with no
335 contribution from pedogenesis.

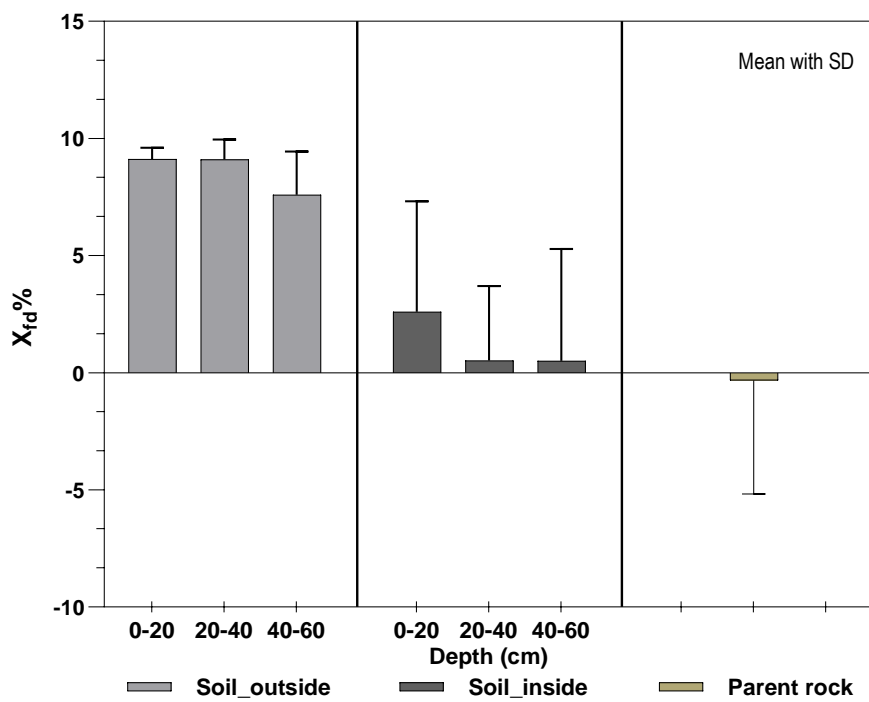


Figure 7. The variation of frequency-dependent magnetic susceptibility ($\chi_{fd}\%$) of soil samples collected from three different categories and depths.

340 **4 Discussions**

Landslide-induced soil degradation is assessed through the hypothesis that landslide processes cause systematic changes in soil physico-chemical properties, increase parameter variability between disturbed and undisturbed soils, and can be effectively diagnosed using functional soil indicators.



4. 1 Impact of landslide processes on soil physico-chemical properties

345 Bulk density, defined as the dry mass of soil per unit volume, is determined by the proportion of pore space relative to solid material. It plays a fundamental role in regulating the storage and movement of air, water, and solutes within the soil, thereby directly influencing properties such as porosity and water availability (Abdelbaki, 2018). These physical attributes significantly affect soil hydrology (Dam et al., 2005), root development, and overall crop productivity (Reichert et al., 2009). Additionally, bulk density is critical for estimating soil water retention characteristics and is widely used in models that simulate water and
350 nutrient transport, plant growth dynamics, and carbon stocks estimation (Walter et al., 2016; Martin et al., 2017; Tian et al., 2021). As such, bulk density serves as a key indicator of grassland ecosystem functionality (Niu et al., 2024). In degraded grassland ecosystem, bulk density typically increases in parallel with the degree of degradation (Wang et al., 2022). This trend is attributed to factors such as reduced vegetation cover, decreased soil organic carbon and moisture content, and anthropogenic pressures like overgrazing, all of which contribute to soil compaction and structural decline (Nawaz et al., 2013). In the present
355 study, bulk density generally exhibits an increasing trend with soil depth. Samples collected outside the landslide area exhibited slightly lower bulk density values compared with those from within the landslide zone, suggesting improved soil aggregation and potentially higher organic matter content in the undisturbed soils (Sher et al., 2022). However, deviations from this pattern were observed at several locations in the central part of landslide area, likely due to the mixing of soil horizons caused by mass movement during the landslide event. Overall, the measured bulk density values were substantially higher than the European
360 average for topsoil (1.03 g/cm³ at 0-20 cm depth), even in samples collected outside the landslide-affected zone. Comparable bulk density values exceeding 1.4 g/cm³ have been reported in other landslides-affected regions, such as the Kutupalong Camp in Bangladesh (Kamal et al., 2022) and the western Himalayas (Habib et al., 2025). These high values are primarily attributed to the mechanical disturbance associated with landslide activity (the high-density parent material is brought to the surface) and secondarily to anthropogenic factors such as high livestock density, intensive grazing pressure, and rainfall patterns. It is well
365 established that in intensively managed pasture systems, repeated animal trampling significantly contributes to soil compaction (Pulido et al., 2018; De Rosa et al., 2020). Soil compaction in such environments directly impacts soil bulk density and has adverse effects on key soil physical properties, including hydraulic conductivity, aeration, macropore volume, and penetration resistance (Hamza and Anderson, 2005).

Soil pH is an important parameter that influences a large range of soil properties and biogeochemical processes, including
370 nutrient cycling and soil fertility (Robinson et al., 2017), microbial activity (Kemmitt et al., 2006), and the decomposition of organic matter (Kölbl et al., 2017; Miller and Kissel, 2010). Due to its integrative role, soil pH serves as a valuable indicator for monitoring land degradation processes, which may adversely impact nutrient availability, promote soil acidification or salinization, and alter chemical conditions that affect both soil biota and plant root function (Hartemink and Barrow, 2023). According to the pH classification proposed by Batjes (1995), the analyzed soil samples generally fall within the slightly to
375 moderately alkaline range. Three exceptions were observed at the 40-60 cm depth interval, where pH values indicated strongly alkaline conditions. In contrast, samples representing the parent material exhibited a broader pH spectrum, ranging from



moderately acidic to strongly alkaline. The pH difference between the soil and the underlying parent material (generally lower in the latter) likely reflects reduced biological buffering capacity and lower organic matter activity (Alfaro et al., 2017; Kowalska et al., 2021). These contrasts were more pronounced than the pH variations between soil samples collected inside 380 and outside the landslide area. Nonetheless, the samples collected outside the landslide area showed slightly higher pH values. This finding contrasts with the results of Cheng et al. (2016), who reported increased pH levels caused by landslide deposition, as well as with Van Eynde et al. (2017), who found no significant differences between the landslide and adjacent fields. Landslides occurring in clay-rich soils are widespread and characterized by a wide range of sizes, morphologies, and kinematic 385 behaviours (Maquaire et al., 2003; Chambers et al., 2011). Some intrinsic properties of clay (high viscosity, strong adsorption capacity and a high plasticity index) are critical in influencing landslide dynamics (Meisina, 2006). The landslides mechanism is highly dependent by mineralogical composition of clays (Azañón et al., 2010), such as smectites, a group with high plasticity 390 and swelling potential which experience periodic swelling and shrinkage during wet and dry seasons (Day, 1994). These alternating cycles of swelling-shrinking are considered critical for the stability of natural slopes together with the moisture content, both being considered as a trigger mechanism in those areas with high-plasticity materials (Yilmaz and Karacan, 395 2002). In the current study, most of the analyzed samples exhibited a clay content exceeding 30%, with the exception of one parent material sample, which had a lower clay content of 19.44%. This confirms that the sampled soils can generally be classified as clay-rich. A higher clay content in surface and subsoil layers, may be attributed to pedogenic processes such as weathering and illuviation processes, which promote clay accumulation. An overall increase in clay content with depth, from topsoil to parent material, was observed in undisturbed profiles. However, this vertical distribution pattern is disrupted in 400 locations affected by landslide activity, where soil horizons have been mixed due to mass movement.

Electrical conductivity is fundamental soil property that responds sensitively to variations in soil moisture showing strong 405 correlation not only with volumetric water content (Ratshiedana et al., 2006), but more precisely with soil water potential (Qin et al., 2020). It is also influenced by a suite of other soil properties, such as bulk density, texture components (clay, silt, and sand), cation-exchange capacity, as well as topographic factors such as elevation and slope (Jung et al., 2005). By comparison, studies on landslide-impacted soils elsewhere have reported lower nutrient concentrations and slower soil quality recovery in disturbed sites, in part due to the loss or dilution of fine mineral fractions and organic matter (Goyal et al., 2022). Our EC data complement these findings, suggesting that while landslide zones may accumulate salinity (ion-rich parent material), they may simultaneously lose or redistribute critical soil quality indicators, such as organic matter. These chemical transformations have potentially significant consequences. Elevated EC can affect soil hydraulic behaviour, retention, and stability. Previous 410 geotechnical and geophysical studies have linked high ion concentrations to zones of low shear strength that favor sliding (Olabode and San, 2023). Thus, higher content and depth-homogenized EC inside the landslide, contrasted with lower and stratified EC in stable soils, underscores how mass movement can override pedogenic gradients, promote ion accumulation from parent material and potentially compromise post-landslide soil stability.

Soil organic matter is an essential component of the soil, exerting a critical influence on their physical, chemical, and biological 415 functioning and regulating the behaviour of other soil components. Our results reveal a marked reduction in soil organic matter



within the landslide-affected zone relative to stable reference soils, confirming the findings of other studies. For example, Blónska et al. (2018) observed significantly lower soil organic carbon and microbial biomass in landslide niches compared to more stable zones, even several years after slope failure, indicating a delayed recovery of organic matter and biological activity. Similarly, work on landslide-disturbed soils in younger or unstable slopes has reported reduced soil quality indices, including 415 diminished soil organic carbon, immediately following mass-wasting events (Van Eynde et al., 2017). Mechanistically, our results suggest that landslide processes disrupt the accumulation of surface organic inputs (e.g., litter and roots) by mixing them with deeper, low-carbon material, thereby decreasing the overall OM content. Over time, this disruption may compromise soil structure and fertility, since organic matter is crucial for aggregation, water retention, and nutrient cycling.

The magnetic behaviour of soils is governed by the mineralogical composition, concentration, and grain size distribution of 420 magnetic minerals (Peters and Dekkers, 2003). Soil magnetic susceptibility is primarily controlled by minerals that originate from three principal sources: lithogenic - derived from parent material; pedogenic - formed through physical, chemical, and biological processes within the soil; and anthropogenic - typically represented by spherical particles from industrial emissions (Ouallali et al., 2025). Variations in the concentration of iron oxides, and consequently in the magnetic susceptibility of soils, are influenced not only by the parent material, physicochemical properties, soil age, temperature, biological activity, and 425 pedogenic transformations, but also by anthropogenic inputs (Shirzaditabar and Heck, 2021). The results of the current study provide compelling evidence that landslide activity substantially alters the soil magnetic mineralogy and pedogenic development, particularly in the upper soil horizons. The contrast in mass-specific magnetic susceptibility among soils outside the landslide, soils inside the landslide, and the parent material illustrates a clear disruption of normal soil formation processes. The decreasing trend of MS with depth in soils outside the landslide aligns with many studies where pedogenic processes 430 enrich the upper horizons with finer ferrimagnetic minerals. For example, Ouallali et al., 2025 show similar patterns where χ_{lf} decreases with depth in well-developed soils, and high χ_{fd}^0 in upper layers indicates accumulation of superparamagnetic particles (SP) under undisturbed conditions. The uniformly low MS values inside the landslide ($\sim 15 \times 10^{-8} \text{ m}^3/\text{kg}$), and similarity to parent material ($\sim 10 \times 10^{-8} \text{ m}^3/\text{kg}$) suggest that the landslide has removed, mixed, or buried the SP-rich topsoil. This corresponds with observations from other works where soil truncation or erosion causes loss of magnetic enhancement 435 (i.e., reduction in frequency-dependent susceptibility) in disturbed soils. For instance, Grison et al., (2017) found that disturbed or poorly developed soils have a much lower SP signal because pedogenic SP minerals are either removed or mixed with deeper, non-pedogenic materials. The very low MS and negative or negligible χ_{fd}^0 values in parent material confirm the idea that SP contributions are minimal in unweathered geological material, where ferrimagnetic mineral grains are coarser (multidomain MD) or dominated by non-SP minerals. This is consistent with findings of Szuszkiewicz et al. (2021) that 440 revealed that parent rock or geogenic material shows little to no SP signal, and the MS is dominated by large, stable MD ferrimagnetic grains. In terms of soil fertility and ecosystem function, the removal or loss of SP-rich horizons can imply loss of fine iron oxides, organic matter associations, and moisture retention capacity, which are crucial for plant root growth, nutrient cycling, and overall soil health (Yu et al., 2024). From a geomorphological and hazard assessment perspective, magnetic property analyses can be integrated with erosion models or landscape stability assessments to evaluate the frequency



445 with which landslide events disrupt soil pedogenesis, as well as the timescale required for post-disturbance magnetic enhancement (i.e. SP accumulation) to reestablish. However, given the cross-sectional nature of this study, it remains challenging to constrain the timing of past disturbances and to quantify the extent or rate of subsequent pedogenic recovery.

4.2 Soil parameter variability in relation to landslide impact - a comparative analysis

450 The comparative assessment of soil from landslide-affected and unaffected areas revealed both subtle and statistically significant variations across several key parameters. In particular, EC, OM and MS exhibited consistently higher values within the landslide zones (Fig. 3 and 5) compared to adjacent undisturbed soils and the underlying parent material. These increases likely reflect the mechanical disruption of soil horizons and the consequent redistribution of organic matter, fine particles and nutrients caused by slope movement, consistent with previous findings on soil perturbation and post-landslide pedogenesis (McKenna et al., 2011). The significantly higher bulk density in landslide-affected soils can be attributed to compaction during 455 slope failure and the collapse of soil aggregates. Such changes reflect the exposure of denser subsoil horizons, reduced porosity and smaller macropores volume, in one case a ~20% increase in bulk density from topsoil to subsoil was observed in a landslide profile in South Africa (Kotzé et al., 2020). This interpretation aligns with findings by Cheng et al. (2016), Bălc et al. (2020) and others who reported similar structural disruptions and declines in soil OM in landslide scars. Mechanical mixing and inversion of horizons therefore appear to be key processes shaping post-failure soil profiles and influencing the redistribution 460 of pedogenic constituents.

Moreover, mass movement may selectively transport fine particles (silt+clay) and organic matter downslope, thereby altering texture and nutrient-holding capacity in the landslide zone (Blońska et al., 2018). In contrast, parameters such as pH and clay content showed no significant differences between disturbed and reference areas. These results may reflect the relatively short period since the landslide event or the inherent resilience of certain soil attributes to physical disturbance. The limited 465 variability in pH further suggests that the soils' buffering capacity remained largely intact despite structural alteration, though minor deviations beyond the landslide area may reflect leaching or dilution effects linked to sediment redistribution.

Chronosequence investigations show that immediately after a slope-failure event, physical attributes (bulk density, porosity) dominate soil response, whereas the longer-term recovery of chemical and biological soil properties (aggregate stability, microbial biomass) proceeds more slowly (Van Eynde et al., 2017). The absence of significant differences in some parameters 470 supports earlier observations, which noted minimal alteration in soil chemistry between landslide and adjacent sites. These findings highlight the complexity of soil–landslide interactions, governed by factors such as landslide type, magnitude, depth of failure and time since disturbance. Such physical and chemical alterations have important implications for soil hydrological and nutrient-cycling dynamics, and ultimately for ecosystem recovery and slope-stability feedbacks. Overall, the results emphasize the need to integrate statistical analyses with process-based understanding to accurately interpret how landslides 475 influence soil quality, functionality and long-term pedogenic development.



4.3 Soil functional indicators as diagnostic tools for land degradation assessment

Identifying reliable soil functional indicators is essential for quantifying the extent and severity of land-degradation processes, as these indicators reflect alterations in key soil functions such as nutrient cycling, water retention and structural stability (Bünemann et al., 2018). In this study, the soil properties that demonstrate a strong diagnostic potential are bulk density, 480 organic matter content, soil CE, and magnetic susceptibility. These parameters cover physical, chemical, and magnetic markers of disturbance, providing a multidimensional assessment of the degradation processes associated with landslide activity and other geomorphic or anthropogenic stressors.

Bulk density emerged as a particularly robust indicator, with higher values consistently recorded in degraded or landslide-affected areas. High values of bulk density indicate compaction due to mechanical disturbance, sediment displacement, or 485 livestock trampling, leading to reduced porosity, infiltration capacity, and root penetration (Hamza and Anderson, 2005; De Rosa et al., 2020). Compaction has been widely recognized as a key physical degradation mechanism that limits soil aeration and water movement, accelerating surface runoff and erosion (Zhang et al., 2006). Therefore, bulk density can effectively capture the mechanical imprint of both anthropogenic and geomorphic stressors, making it a reliable early-warning indicator in vulnerable landscapes.

490 Organic matter content also proved to be a sensitive and integrative indicator of soil degradation. OM was significantly lower in disturbed profiles, consistent with organic matter loss through erosion, oxidation, and diminished biological input. As organic matter underpins aggregate stability, nutrient retention, and microbial functioning, its depletion signals both chemical and biological degradation (Lal, 2004). The observed spatial variability in OM reflects heterogeneity in disturbance intensity and topsoil removal, highlighting the importance of landscape context when interpreting degradation patterns. Beyond 495 reflecting loss, OM dynamics can provide insight into the recovery potential and the resilience of the soil's functional processes.

EC emerges as a particularly informative functional indicator for diagnosing land degradation in landslide-affected terrains. Its strong sensitivity to soil water content is well established, with EC exhibiting predictable increases in response to higher 500 moisture levels and the presence of fine-textured mineral fractions, which collectively enhance the continuity of conductive pathways within the soil matrix (Ylagan et al., 2022). This parameter is also influenced by bulk density and ion content because these parameters affect the continuity and conductivity of pathways (Hossain et al., 2018). The observed pattern of EC values in our study clearly indicate that the mass movement disrupted natural stratification, mobilized ion-rich parent material while simultaneously redistributing or depleting components key to the soil's quality components. Thus, EC, when interpreted alongside complementary physical and chemical indicators, provides a robust diagnostic lens for identifying both the depth 505 and the trajectory of functional degradation in landslide-impacted soils.

Among the less conventional yet highly informative functional indicators, magnetic susceptibility (MS) and its frequency-dependent component ($\chi_{fd\%}$) effectively distinguished soils outside landslide zones from those within or from underlying parent material. Reduced $\chi_{fd\%}$ and MS in disturbed soils reflect the physical removal or homogenization of the pedogenically



enriched topsoil, leaving magnetic properties that more closely resemble unaltered parent substrates. This finding underscores
510 the potential of environmental magnetism as a rapid, non-destructive diagnostic tool for identifying disturbed zones, quantifying topsoil loss, and assessing the degree of soil formation or degradation. Moreover, magnetic properties provide a unique link between mineralogical changes and functional soil processes, complementing physical and biochemical indicators. Overall, the combined use of bulk density, OM, and magnetic parameters provides a reliable and sensitive framework for
515 diagnosing land degradation in geomorphically active landscapes. These indicators integrate the physical, biochemical, and mineralogical dimensions of soil functioning, enabling robust assessment of both process intensity and recovery potential. Their inclusion in multi-indicator monitoring systems could substantially improve early detection of degradation, support targeted restoration planning, and enhance land management strategies in erosion-prone or landslide-affected terrains. Future work should aim to validate these indicators across broader spatial scales and diverse climatic and land-use contexts to strengthen their general applicability in soil health assessment.

520 **5 Conclusions**

This study provides an integrated assessment of soil quality dynamics across a complete landslide profile in the Transylvanian Basin, allowing the identification of the soil properties most altered by landslide activity. The results demonstrate that electrical conductivity, organic matter content, and magnetic susceptibility are the parameters most strongly affected, reflecting the mechanical disturbance, compaction, and material mixing induced by slope failure. Statistically significant contrasts between
525 landslide-affected and intact soils were observed for most analysed attributes, confirming that mass movement disrupts natural vertical gradients, reduces pedogenic development, and enhances solute accumulation. Among all parameters, magnetic susceptibility (both mass-specific and frequency-dependent), organic matter, and electrical conductivity emerged as the most diagnostically relevant indicators for evaluating soil disturbance severity and landscape degradation. Overall, the study highlights the utility of combined physico-chemical and magnetic analyses for detecting landslide impacts, offering a robust
530 framework for assessing soil quality deterioration in geomorphologically dynamic terrains.

In summary, this study demonstrates how landslides reshape soil systems and identifies key diagnostic parameters essential for assessing disturbance severity. These insights contribute to a deeper understanding of landscape evolution and offer a framework applicable to other landslide-prone regions.

Code, data, or code and data availability

535 The raw data underlying this study are not publicly available. However, we consider the raw data sufficient for evaluating the manuscript, and they will be provided to reviewers upon request through the Copernicus review system under restricted access.



Author contributions

Conceptualization, G.R. and R.B.; methodology, G.R., R.B., R.M., S.S., T.O., C.H. and T.B.; software, G.R., R.B., T.O., C.H. and T.D.; validation, G.R., R.B., T.O. and C.A.R.; formal analysis, R.B., R.M. and S.S.; investigation, G.R., R.B., R.M. and S.S.; writing—G.R. and R.B.; writing—review and editing, G.R., R.B., R.M., T.O. and C.H.; visualization, G.R., R.B., R.M., T.O., C.H. and T.D.; supervision, G.R. and R.B. All authors have read and agreed to the published version of the manuscript.

Competing interests

The authors declare no conflicts of interest.

Acknowledgements

545 The authors sincerely thank the colleagues who supported both the fieldwork and the laboratory analyses. Their commitment, technical assistance, and teamwork were essential to the completion of this study.

Financial support

This research received no external funding.

550 References

Abdelbaki, A. M.: Evaluation of pedotransfer functions for predicting soil bulk density for U.S. soils, *Ain Shams Engineering Journal*, 9, 1611-1619, <https://doi.org/10.1016/j.asej.2016.12.002>, 2018.

Alfaro, F., Manzano, M., Marquet, P. A., and Gaxiola, A.: Microbial communities in soil chronosequences with distinct parent material: the effect of soil pH and litter quality, *Journal of Ecology*, 105, 1709-1722, <https://doi.org/10.1111/1365-2745.12766>, 2017.

Azañón, J. M., Azor, A., Yesares, J., Tsige, M., Mateos, R. M., Nieto, F., Delgado, J., López-Chicano, M., Martín, W., and Rodríguez-Fernández, J.: Regional-scale high-plasticity clay-bearing formation as controlling factor on landslides in Southeast Spain, *Geomorphology*, 120, 26-37, <https://doi.org/10.1016/j.geomorph.2009.09.012>, 2010.

Bălc, R., Roba, C., Roşian, G., Costin, D., Horvath, C., Zglobiu, O. R., and Chirtoş, D.: Changes in the physico-chemical properties of topsoil in a landslide-affected area (western part of the Transylvanian Basin, Romania), *Geological Quarterly*, 64, 931-941, <http://dx.doi.org/10.7306/gq.1561>, 2020.



Bălteanu, D., Micu, M., Jurchescu, M., Malet, J.-P., Sima, M., Kucsicsa, G., Dumitrică, C., Petrea, D., Mărgărint, M. C., Bilașco, S., Dobrescu, C.-F., Călărașu, E.-A., Olinic, E., Boți, I., and Senzaconi, F.: National-scale landslide susceptibility map of Romania in a European methodological framework, *Geomorphology*, 371, 107432, 565 <https://doi.org/10.1016/j.geomorph.2020.107432>, 2020.

Batjes, N. H.: A global data set of soil pH properties, Technical Paper 27, International Soil Reference and Information Centre (ISRIC), Wageningen, 1995.

Błońska, E., Lasota, J., Piaszczyk, W., Wiecheć, M., and Klamerus-Iwan, A.: The effect of landslide on soil organic carbon stock and biochemical properties of soil, *Journal of Soil and Sediments*, 18, 2727-2737, <https://doi.org/10.1007/s11368-017-1775-4>, 2018.

Boushane, N. and Bouhlassa, S.: Assessing magnetic susceptibility profiles of topsoils under different occupations, *International Journal of Geophysics*, 2018, 1-8, <https://doi.org/10.1155/2018/9481405>, 2018.

Bünemann, E. K., Bongiorno, G., Bai, Z., Creamer, R. E., De Deyn, G., de Goede, R., Fleskens, L., Geissen, V., Kuyper, T. W., Mäder, P., Pulleman, M., Sukkel, W., van Groenigen, J. W., and Brussaard, L.: Soil quality—A critical review, *Soil Biology and Biochemistry*, 120, 105-125, <https://doi.org/10.1016/j.soilbio.2018.01.030>, 2018.

Cerri, R. I., Rosolen, V., Reis, F. A. G. V., Filho, A. J. P., Vemado, F., Giordano, L. C., and Gabelini, B. M.: The assessment of soil chemical, physical, and structural properties as landslide predisposing factors in the Serra do Marmountain range (Caraguatatuba, Brazil), *Bulletin of Engineering Geology and the Environment*, 79, 3307-3320 <https://doi.org/10.1007/s10064-020-01791-1>, 2020.

Chambers, J. E., Wilkinson, P. B., Kuras, O., Ford, J. R., Gunn, D. A., Meldrum, P. I., Pennington, C. V. L., Weller, A. L., Hobbs, P. R. N., and Ogilvy, R. D.: Three-dimensional geophysical anatomy of an active landslide in Lias Group mudrocks, Cleveland Basin, UK, *Geomorphology*, 125, 472-484, <https://doi.org/10.1016/j.geomorph.2010.09.017>, 2011.

Cheng, C.-H., Hsiao, S.-C., Huang, Y.-S., Hung, C.-Y., Pai, C.-W., Chen, C.-P., and Menyailo, O. V.: Landslide-induced changes of soil physicochemical properties in Xitou, Central Taiwan, *Geoderma*, 265, 187-195, 580 <https://doi.org/10.1016/j.geoderma.2015.11.028>, 2016.

Ciulavu, D. and Bertotti, G.: The Transylvanian Basin and its Upper Cretaceous substratum: ALCAPA II Field Guidebook, *Romanian Journal of Tectonics and Regional Geology* 75, 59–65, 1994.

Ciulavu, D., Dinu, C., Szakács, A., and Dordea, D.: Neogene kinematics of the Transylvanian basin (Romania), *AAPG Bulletin*, 84, 1589-1615, <https://doi.org/10.1306/8626BF0B-173B-11D7-8645000102C1865D>, 2000.

Ciupagea, D., Păucă, M., and Ichim, T.: Geology of the Transylvanian Depression (in Romanian), Acad. R.S.R, Bucharest, 256 pp., 1970.

Cruden, D. M. and Varnes, D. J.: Landslide types and processes, in: *Landslides Investigation and Mitigation*, edited by: Turner, A. K. and Schuster, R. L., Transportation Research Board, Special Report, 247, National Research Council, National Academy Press, Washington, D.C., pp. 36–75, 1996.



595 Dam, R. F., Mehdi, B. B., Burgess, M. S. E., Madramootoo, C. A., Mehuys, G. R., and Callum, I. R.: Soil bulk density and crop yield under eleven consecutive years of corn with different tillage and residue practices in a sandy loam soil in central Canada, *Soil & Tillage Research*, 84, 41-53, <https://doi.org/10.1016/j.still.2004.08.006>, 2005.

Day, R. W.: Swell-Shrink Behavior of Compacted Clay, *Journal Geotechnical Engineering*, 120, 618–623, 1994.

Dean, W. E. Jr.: Determination of carbonate and organic matter in calcareous sediments and sedimentary rocks by loss on ignition: Comparison with other methods, *Journal of Sedimentary Petrology*, 44, 242–248. <https://doi.org/10.1306/74d729d2-2b21-11d7-8648000102c1865d>, 1974.

de Broucker, G., Mellin, A., and Duindam, P.: Tectono-Stratigraphic evolution of the Transylvanian Basin, pre-salt sequence, Romania, in: Geological and Hydrocarbon Potential of the Romanian Areas, edited by: Dinu, C. and Mocanu, V., Bucharest Geosciences Forum Special Volume, vol. 1, pp. 36–70, 1998.

605 De Rosa, D., Rowlings, D. W., Fulkerson, B., Scheer, C., Friedl, J., Labadz, M., and Grace, P. R.: Field-scale management and environmental drivers of N₂O emissions from pasture-based dairy systems, *Nutrient Cycling in Agroecosystem*, 117, 299-315, <https://doi.org/10.1007/s10705-020-10069-7>, 2020.

Dean, W. E. Jr.: Determination of carbonate and organic matter in calcareous sediments and sedimentary rocks by loss on ignition: Comparison with other methods, *Journal of Sedimentary Petrology*, 44, 242–248, <https://doi.org/10.1306/74d729d2-2b21-11d7-8648000102c1865d>, 1974.

610 Doran, J. W. and Parkin, T.B.: Quantitative indicators of soil quality: a minimum data set, in: *Methods for Assessing Soil Quality*, edited by: Doran, J. W. and Jones, A. J., Soil Science Society of America (SSSA) Special Publ., 49, Madison, WI. p. 25–39, <https://doi.org/10.2136/sssaspecpub49.c2>, 1996.

Doran, J. W. and Zeiss, M. R.: Soil health and sustainability: managing the biotic component of soil quality, *Applied Soil Ecology*, 15, 3-11, [https://doi.org/10.1016/S0929-1393\(00\)00067-6](https://doi.org/10.1016/S0929-1393(00)00067-6), 2000.

615 Foth, H. D.: *Fundamentals of Soil Science*, Eighth ed., Wiley & Sons, New York, 360 p., 1991.

Geertsema, M., Highland, L., and Vaugeouis, L.: Environmental impact of landslides, in *Landslides – disaster risk reduction*, edited by: Sassa, K. and Caneti, P., Springer-Verlag Berlin Heidelberg, 2009.

Goyal, D., Joshi, V., Gupta, N., and Cabral-Pinto, M. M. S.: Soil quality assessment in a landslide chronosequence of Indian 620 Himalayan region, *Land*, 11, 1819. <https://doi.org/10.3390/land11101819>, 2022.

Grison, H., Petrovsky, E., Kapicka, A., and Hanzlikova, H.: 2017. Detection of the pedogenic magnetic fraction in volcanic soils developed on basalts using frequency-dependent magnetic susceptibility: comparison of two instruments, *Geophysical Journal International*, 209, 654-660, doi:10.1093/gji/ggx037, 2017.

Habib, Z., Kumar, A., Mir, R. A., Bhat, I. M., Qader, W., and Mallik, R. K.: Geotechnical analysis and landslide susceptibility 625 of overburden slope material in the Jammu and Kashmir, Western Himalaya, *Geosystems and Geoenvironment*, 4, 100413, <https://doi.org/10.1016/j.geogeo.2025.100413>, 2005.

Hamza, M. A., Anderson, W. K.: Soil compaction in cropping systems A review of the nature, causes and possible solutions, *Soil & Tillage Research*, 82, 121-145, <https://doi.org/10.1016/j.still.2004.08.009>, 2005.



Hartemink, A. E. and Barrow, N. J.: Soil pH – nutrient relationships: the diagram, *Plant and Soil*, 486, 209-215,
630 https://doi.org/10.1007/s11104-022-05861-z, 2003.

Heiri, O., Lotter, A. F., and Lemcke, G.: Loss on ignition as a method for estimating organic and carbonate content in sediments: reproducibility and comparability of results, *Journal of Paleolimnology*, 25, 101-110, <https://doi.org/10.1023/A:1008119611481>, 2001.

Hossain, M. S., Rahman, G. K. M. M., Alam, M.S., Rahman, M.M., Solaiman, A. R. M., and Mia, M. A. B.: Modelling of soil texture and its verification with related soil properties, *Soil Research*, 56(4), 421-428, <https://doi.org/10.1071/SR17252>, 2018.

Huismans, R. S., Bertotti, G., Ciulavu, D., Sanders, C. A. E., Cloetingh, S., and Dinu, C.: Structural evolution of the Transylvanian Basin (Romania): a sedimentary basin in the bend zone of the Carpathians, *Tectonophysics* 272, 249–268, [https://doi.org/10.1016/S0040-1951\(96\)00261-2](https://doi.org/10.1016/S0040-1951(96)00261-2), 1997.

International Organization for Standardization (ISO): ISO 11272:2017 – Soil quality: Determination of dry density and water content for soil in the field, Geneva, ISO, 2017.

640 Jung, W. K., Kitchen, N. R., Sudduth, K.A., Kremer, R. J., and Motavalli, P. P.: Relationship of Apparent Soil Electrical Conductivity to Claypan Soil Properties, *Soil Science Society of America Journal*, 69, 883-892, doi:10.2136/sssaj2004.0202, 2005.

Kamal, A. S. M. M., Hossain, F., Rahman, M. Z., Ahmed, B., and Sammonds, P.: Geological and soil engineering properties of shallow landslides occurring in the Kutupalong Rohingya Camp in Cox's Bazar, Bangladesh, *Landslides*, 19, 465-478, <https://doi.org/10.1007/s10346-021-01810-6>, 2022.

Kemmit, S. J., Wright, D., Goulding, K. W. T., and Jones, D. L.: pH regulation of carbon and nitrogen dynamics in two agricultural soils, *Soil Biology & Biochemistry*, 38, 898-911, <https://doi.org/10.1016/j.soilbio.2005.08.006>, 2006.

Kölbl, A., Marschner, P., Fitzpatrick, R., Mosley, L., and Kögel-Knabner, I.: Linking organic matter composition in acid sulfate soils to pH recovery after re-submerging, *Geoderma*, 308, 350-362, <http://dx.doi.org/10.1016/j.geoderma.2017.07.031>, 2017.

Kotzé, J., Le Roux, J., and van Tol, J.: Investigating Soil Properties at Landslide Locations in the Eastern Cape Province, South Africa, *GeoHazards*, 6, 68. <https://doi.org/10.3390/geohazards6040068>, 2025.

Kowalska, J. B., Skiba, M., Maj-Szeliga, K., Mazurek, R., and Zaleski, T.: Does calcium carbonate influence clay mineral transformation in soils developed from slope deposits in Southern Poland? *Journal of Soils and Sediments*, 21, 257-280, <https://doi.org/10.1007/s11368-020-02764-3>, 2021.

Krézsek, C. and Filipescu, S.: Middle to Late Miocene sequence stratigraphy of the Transylvanian Basin (Romania), *Tectonophysics*, 410, 437–463, <https://doi.org/10.1016/j.tecto.2005.02.018>, 2005.

Krézsek, C. and Bally, A. W.: The Transylvanian Basin (Romania) and its relation to the Carpathian Fold and Thrust Belt: 655 insights in gravitational salt tectonics, *Marine and Petroleum Geology*, 23, 405–446, <https://doi.org/10.1016/j.marpetgeo.2006.03.003>, 2006.



Krézsek, C., Adam, J., and Grujic, D.: Mechanics of fault and expulsion rollover systems developed on passive margins detached on salt: insights from analogue modelling and optical strain monitoring, Geological Society, London, Special Publications, 292, 103–121, <https://doi.org/10.1144/SP292.6>, 2007.

665 Lal, R.: Soil carbon sequestration impacts on global climate change and food security, *Science*, 304, 1623–1627, <https://doi.org/10.1126/science.1097396>, 2004.

Maquaire, O., Malet, J.-P., Remaître, A., Locat, J., Klotz, S., and Guillon, J.: Instability conditions of marly hillslopes: towards landsliding or gullyling? The case of the Barcelonnette Basin, South East France, *Engineering Geology*, 70, 109-130, [https://doi.org/10.1016/S0013-7952\(03\)00086-3](https://doi.org/10.1016/S0013-7952(03)00086-3), 2003.

670 Martin M. Á., Reyes, M., and Taguas, F. J.: Estimating soil bulk density with information metrics of soil texture, *Geoderma*, 287, 66-70, 2003, <https://doi.org/10.1016/j.geoderma.2016.09.008>, 2017.

Matei, L.: Pannonian clays of Transylvania (in Romanian), Edit. Academiei, Bucureşti, 160 p., 1983.

McKenna, J. P., Santi, P. M., Amblard, X., and Negri, J.: Effects of soil-engineering properties on the failure mode of shallow landslides, *Landslides*, 9, 215-228, <https://doi.org/10.1007/s10346-011-0295-3>, 2011.

675 Meisina, C.: Characterisation of weathered clayey soils responsible for shallow landslides, *Natural Hazards in Earth System Sciences*, 6, 825-838, 2006.

Miller, R. O. and Kissel, D. E.: Comparison of soil pH methods on soils of North America, *Soil Science Society of America Journal*, 74, 310-316, <https://doi.org/10.2136/sssaj2008.0047>, 2010.

Nawaz, M. F., Bourrié, G., and Trolard, F.: Soil compaction impact and modelling. A review, *Agronomy for Sustainable 680 Development*, 33, 291-309, <https://doi.org/10.1007/s13593-011-0071-8>, 2013.

Niu, W., Ding, J., Fu, B., Zhao, W., Han, Y., Zhou, A., Liu, Y., and Eldridge, D.: Ecosystem multifunctionality is more related to the indirect effects than to the direct effects of human management in China's drylands, *Journal of Environmental Management*, 368, 122259, <https://doi.org/10.1016/j.jenvman.2024.122259>, 2024.

Olabode, O. P. and San, L. H.: Analysis of soil electrical resistivity and hydraulic conductivity relationship for characterisation 685 of lithology inducing slope instability in residual soil, *International Journal of Geo-Engineering*, 14, 7, <https://doi.org/10.1186/s40703-023-00184-z>, 2023.

Quallali, A., Bouhsane, N., Bouhlassa, S., Spalevic, V., Kader, S., Michael, R., and Sestras, P.: Exploring soil pedogenesis through frequency-dependent magnetic susceptibility in varied lithological environments, *Euro-Mediterranean Journal for Environmental Integration*, 10, 887-900, <https://doi.org/10.1007/s41207-024-00663-4>, 2025.

690 Paraschiv, D.: Romanian oil and gas fields, *Tech. and Eco. Stu.*, 13, 382, 1979.

Peters, C. and Dekkers, M. J.: Selected room temperature magnetic parameters as a function of mineralogy, concentration and grain size, *Physics and Chemistry of the Earth*, 28 (16–19), 659 – 667, [https://doi.org/10.1016/S1474-7065\(03\)00120-7](https://doi.org/10.1016/S1474-7065(03)00120-7), 2003.

Pulido, M., Schnabel, S., Contador, J. F. L., Lozano-Parra, J., and González, F.: The impact of heavy grazing on soil quality and pasture production in rangelands of SW Spain, *Land Degradation & Development*, 29, 219-230, 695 <https://doi.org/10.1002/ldr.2501>, 2018.



Qin, P., Liu, Y., Song, Z., Ma, F., Wang, Y., Zhang, X., Miao, C., Dong, X.: An Electrical Resistivity Method of Characterizing Hydromechanical and Structural Properties of Compacted Loess during Constant Rate of Strain Compression, *Sensors* 20(17), 4783, doi:10.3390/s20174783, 2020.

700 Ratshiedana, P. E., Elbasit, M. A. M. A., Adam, E., Chirima, J. G., Liu, G., and Economou, E. B.: Determination of Soil Electrical Conductivity and Moisture on Different Soil Layers Using Electromagnetic Techniques in Irrigated Arid Environments in South Africa, *Water*, 15, 1911, <https://doi.org/10.3390/w15101911>, 2023.

Reichert, J. M., Suzuki, L. E. A. S., Reinert, D. J., Horn, R., and Håkansson, I.: Reference bulk density and critical degree-of-compactness for no-till crop production in subtropical highly weathered soils, *Soil & Tillage Research*, 102, 242-254, <https://doi.org/10.1016/j.still.2008.07.002>, 2009.

705 Robinson, N. J., Benke, K. K., Norng, S., Kitching, M., and Crawford, D. M.: Improving the information content in soil pH maps: a case study, *European Journal of Soil Science*, 68, 592-604, <https://doi.org/10.1111/ejss.12452>, 2017.

Ross, A. and Willson, V. L.: One-Way Anova, in *Basic and Advanced Statistical Tests*, edited by: Ross, A. and Willson, V. L., Sense Publishers, 21–24, https://doi.org/10.1007/978-94-6351-086-8_5, 2017.

710 Roşian, G., Horvath, Cs., Reti, K. O., Boțan, C., and Gavrilă, I.: Assessing landslide vulnerability using bivariate statistical analysis and the frequency ratio model. Case study: Transylvanian Plain, *Zeitschrift für Geomorphologie*, 60(4), 359-371, <https://doi.org/10.1127/zfg/2016/0404>, 2016.

Royden, L.: Late Cenozoic tectonics of the Pannonian Basin system, *AAPG Membranes* 45, 27–48, <https://doi.org/10.1306/M45474C3>, 1998.

715 Sanders, C. A. E., Huismans, R., van Wees, J. D., and Andriessen, P.: The Neogene history of the Transylvanian Basin in relation to its surrounding mountains, *EGU Stephan Mueller Special Publication, Series 3*, 121–133, 2002.

Săndulescu, M.: *Geotectonica României*, Ed. Tehnică, Bucharest, 329 pp., 1984.

Săndulescu, M.: Cenozoic tectonic history of the Carpathians, in: *The Pannonian Basin: a study in basin evolution*, edited by: Royden, L. and Horváth, F., *AAPG Membranes* 45, 17–25, 1988.

720 Sher, A., Adnan, M., Sattar, A., Ul-Allah, S., Ijaz, M., Hassan, M. U., Manaf, A., Qayyum, A., Elesawy, B. H., Ismail, K. A., Gharib, A. F. and Askary, A. E.: Combined Application of Organic and Inorganic Amendments Improved the Yield and Nutritional Quality of Forage Sorghum, *Agronomy*, 12, 896, <https://doi.org/10.3390/agronomy12040896>, 2022.

Shirzaditabar, F. and Heck, R. J.: Characterization of soil magnetic susceptibility: a review of fundamental concepts, instrumentation, and applications, *Canadian Journal of Soil Science*, 102, 231-251, <https://doi.org/10.1139/cjss-2021-0040>, 2022.

725 STAS 1913/5-85, SR EN 14688-2: Determination of Grain Size-Sedimentation and Sift Method, National Standard-Official Edition (in Romanian), Romanian Institute of Standardization, 1–16, 2005.

Szuszkiewicz, M., Grison, H., Petrovský, E., Szuszkiewicz, M.M., Gołuchowska, B., and Łukasik, A.: Quantification of pedogenic particles masked by geogenic magnetic fraction, *Scientific Report*, 11, 14800, <https://doi.org/10.1038/s41598-021-94039-1>, 2021.



730 Tian, Z., Chen, J., Cai, C., Gao, W., Ren, T., Heitman, J. L., and Horton, R.: New pedotransfer functions for soil water retention curves that better account for bulk density effects, *Soil & Tillage Research*, 205, 104812, <https://doi.org/10.1016/j.still.2020.104812>, 2021.

Van Eynde, E., Dondeyne, S., Isabirye, M., Deckers, J., and Poesen, J.: Impact of landslides on soil characteristics: Implications for estimating their age, *Catena*, 157, 173-179, <http://dx.doi.org/10.1016/j.catena.2017.05.003>, 2017.

735 Walter, K., Don, A., Tiemeyer, B., and Freibauer, A.: Determining Soil Bulk Density for Carbon Stock Calculations: A Systematic Method Comparison, *Soil Science Society of America Journal*, 80, 579-591, <https://doi.org/10.2136/sssaj2015.11.0407>, 2016.

Wang, C., Liu, Z., Yu, W., Ye, X., Ma, L., Wang, R., Huang, Z., and Liu, G.: Grassland Degradation Has Stronger Effects on Soil Fungal Community Than Bacterial Community across the Semi-Arid Region of Northern China, *Plants*, 11, 3488, 2022.

740 Yilmaz, I. and Karacan, E.: A Landslide in clayey soils: an example from the Kızıldag region of the Sivas-Erzincan Highway (Sivas-Turkey), *Environmental Geosciences*, 9, 35-42, <https://doi.org/10.1046/j.1526-0984.2002.91002.x>, 2002.

Ylagan, S., Brye, K. R., Ashworth, A. J., Owens, P. R., Smith, H., and Poncet, A. M.: Using apparent electrical conductivity to delineate field variation in an agroforestry system in the Ozark Highlands, *Remote Sensing*, 14, 5777, <https://doi.org/10.3390/rs14225777>, 2022.

745 Yu, C., Luong, N.T., Hefni, M. E., Song, Z., Högfors-Rönnholm, E., Engblom, S., Xie, S., Chernikov, R., Broström, M., Boily, J.-F., and Åström, M. E.: Storage and distribution of organic carbon and nutrients in acidic soils developed on sulfidic sediments: the roles of reactive iron and macropores, *Environmental Science & Technology*, 58, 9200-9212. <https://doi.org/10.1021/acs.est.3c11007>, 2024.

Zhang, S., Grip, H., and Lövdahl, L: Effect of soil compaction on hydraulic properties of two loess soils in China, *Soil & Tillage Research*, 90, 117-125. doi:10.1016/j.still.2005.08.012, 2006.